Trajectory Planning for Motion-Constrained AUVs in Uncertain Environments

Sarah E. Houts
Stanford University
Department of Aeronautics and Astronautics
Email: shouts@stanford.edu

Stephen M. Rock
Stanford University
Department of Aeronautics and Astronautics
Email: rock@stanford.edu

***Abstract*—Providing a series of images of a site over time with a survey-class AUV presents numerous challenges, particularly in the process of getting close to rugged terrain with a motion-constrained vehicle in an uncertain environment. To deal with this, a baseline approach presented in previous work by the authors plans spline-based trajectories based on an *a priori* map of the terrain, allowing for improved performance over purely reactive control schemes. This paper extends that approach to account for uncertainty in the environment, both in the knowledge of the terrain and the motion of the vehicle, providing additional robustness and safety, while minimizing the potential loss in performance. The trajectory optimization approach is demonstrated over simulated terrain.**

I. Introduction

A motivating mission for Autonomous Underwater Vehicles (AUVs) is to collect a series of images of a site over time to monitor it for change. In order to perform such a return-to-site mission, the vehicle must be able to navigate back to the site of interest, then drop down close to the terrain to gather images.

Terrain-Relative Navigation (TRN) has made the navigation task possible in recent years, allowing the vehicle to return within a few meters of a site of interest by navigating with respect to an onboard *a priori* map of the terrain [1], [2], [3].

However, imaging the sea floor with an AUV presents several challenges. Because sites of interest can be far from the AUV's launch point, an AUV optimized for range, or survey-class, may often be used. The result of this is that the AUV will likely have limited maneuverability (e.g. large turning radius and limited pitch capability). An example of such a vehicle is shown in Figure 1, one of the Monterey Bay Aquarium Research Institute's (MBARI) *Dorado*-class AUVs. These motion contraints create a significant challenge in rugged terrain when the AUV must fly within only a few meters of the sea floor in order to achieve sufficient illumination of the terrain for a visible wavelength camera (e.g. due to the turbidity of the water).

Another challenge to imaging the terrain safely is that there will be uncertainties in the *a priori* knowledge of the environment as well as in the trajectory actually flown by the AUV. That is, there will be uncertainty in the map of the terrain and the model of the AUV used to compute the planned paths as well as unknown disturbances acting on the AUV.

A demonstrated approach to maintaining the safety of the AUV is to fly reactively, using a forward-looking sonar to observe the terrain ahead [4], [5]. However, such reactive approaches are often overly conservative, as they do not take advantage of any prior knowledge. This can result in large sections of terrain not being imaged.

Fig. 1. A *Dorado*-class AUV at MBARI.

Previous work by the authors [6] demonstrated that planning trajectories using *a priori* map data can provide a significant improvement in performance over purely reactive control schemes. The approach described there involved an optimization problem to plan spline-based trajectories that were constrained to satisfy motion constraints.

However, the previous approach assumed perfect knowledge of the environment, making it vulnerable to unmodeled uncertainty in the environment that could lead to violations of the minimum altitude safety constraints. See Figure 4.

This paper extends that previous work to include uncertainty in the optimzation in order to improve robustness and safety. This new approach is based on the work on chance constraints found in [7], modified for use with the spline trajectory implementation.

II. Baseline Approach

The trajectory planning approach presented in [6] uses a uni-parametric spline to define the trajectory, which is constrained to be both safe and feasible.

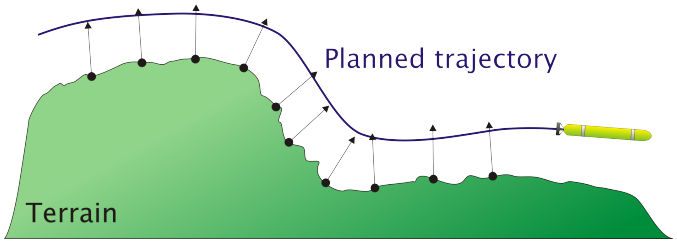

Fig. 2. A depiction of the planned trajectory over the terrain. Points are moved to the desired standoff distance, then the trajectory is planned to fit them as closely as possible while observing the motion and safety constraints.

Splines are chosen because they provide a smooth, easily differentiable trajectory that requires the determination of a smaller set of parameters (i.e. the control points) than the number of data points, reducing the required computation and allowing this approach to be implemented online. Further, trajectories can be planned through any sequence of 3D points, allowing this approach to plan trajectories using data from either an *a priori* map or a local terrain profile measured by onboard sensors.

A uni-parametric spline can be written as follows,

$$\begin{aligned} C &= NP \\ C^{(1)} &= AP \\ C^{(2)} &= BP, \end{aligned}$$

where C is the spline curve, $C^{(j)}$ its jth derivative, P are the control points, N are the basis functions, and A and B are the first and second derivatives of the basis functions respectively. (For a detailed discussion of splines, see [8].)

To calculate a trajectory, a set of data points, d_k, is generated through which the trajectory is desired to pass. The whole set of all k data points is D. In the results shown here, the desired points are generated by taking points from the map of the terrain at approximately one-meter intervals and raising them to the desired standoff distance.

Thus, the goal for the optimization is to find the control points P for which the desired points D are most closely matched. The point on the spline N_kP corresponds to the data point d_k, where N_k represents the basis functions evaluated at the kth point along the spline. At the same time, constraints must be enforced that ensure that the trajectory is still achievable for the motion-constrained vehicle and never gets dangerously close to the terrain. Consequently, motion constraints are placed on the curvature, κ, and the pitch, θ. The safety constraint can be defined as $E < 0$, where E is the margin of safety beyond the minimum standoff distance.

The baseline optimization problem being solved can be written as

$$\begin{aligned} \underset{P}{\text{minimize}} \quad & \|NP - D\| \\ \text{subject to} \quad & \kappa \leq \kappa_{\max} \\ & -\theta_{\max} \leq \theta \leq \theta_{\max} \\ & E > 0. \end{aligned} \tag{1}$$

The constraints are further detailed below, separated into the two categories of motion constraints and safety constraints.

A. Motion Constraints

The vehicles that this work has focused on are survey-class AUVs that have been designed for long distance travel – usually a long, thin cylinder with only a vectored thruster at the rear. As a result, the vehicle is unable to hover and must maintain forward motion in order to retain control authority.

For this type of vehicle, a minimum turning radius is a convenient and effective description of its maneuverability. This minimum turning radius can be expressed as a maximum curvature, $\kappa_{\max} = 1/r_{\min}$, of the spline trajectory. For the AUVs used in the results presented here, the effective turning radius is 17 meters.

Curvature is defined as follows and can be written in terms of the spline parameters.

$$\begin{aligned} \kappa &= \frac{\|C^{(1)} \times C^{(2)}\|}{\|C^{(1)}\|^3} \\ &= \frac{\|AP \times BP\|}{\|AP\|^3}. \end{aligned} \tag{2}$$

The curvature constraint is difficult to implement as written in Equation 2. However, a conservative and more computationally convenient version of the constraint can be expressed as

$$\kappa = \frac{\|AP \times BP\|}{\|AP\|^3} \leq \frac{\|BP\|}{\|AP\|^3} \leq \kappa_{\max} \tag{3}$$

The pitch constraint can be written in terms of the ratio of the vertical component and the magnitude of the first derivative of the spline,

$$\|\sin(\theta)\| = \frac{\|AP(3)\|}{\|AP\|} \leq \sin(\theta_{\max}). \tag{4}$$

Both of these parameterized motion constraints are non-convex, but are written in a form that makes them easily differentiable with respect to the spline control points, P. By squaring the constraints, the Hessian of the Lagrangian can be computed in closed form, enabling efficient solution via interior point methods.

These constraints are enforced at locations all along the spline trajectory.

B. Safety Constraints

As well as ensuring that the trajectories are feasible, they must also respect the minimum standoff distance in order to remain safe.

For the task of bottom following for the imaging mission, the most important safety constraint is ensuring that the vehicle never gets dangerously close to the terrain. This constraint, shown in Figure 3, can be written as

$$E_k = h_k^{\mathsf{T}} \left(N_k P - d_{k,\min}\right) > 0, \tag{5}$$

where E_k is the margin of safety at the kth location, defined as the distance in the direction h_k, which is perpendicular to the terrain, between the point N_kP on the spline and the minimum standoff distance, $d_{k,\min}$.

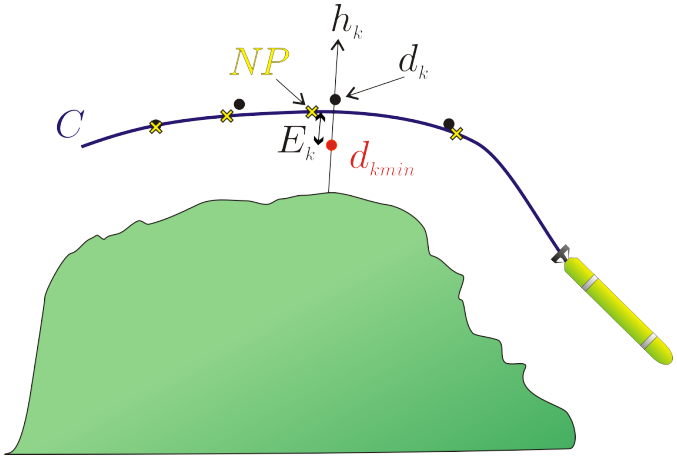

Fig. 3. Minimum standoff distance constraint showing E_k. The trajectory is constrained to keep $E_k > 0$, i.e. outside the minimum standoff distance $d_{k,\text{min}}$.

This implementation provides a hard, deterministic constraint on the minimum standoff distance, between the kth location on the spline and the kth data point. With this implementation, the constraint is linear, allowing it to be solved very quickly within the optimization.

III. Adding Uncertainty

In order to make these planned trajectories more robust to the known sources of uncertainties in the system, uncertainty must be incorporated into the safety constraints. That is, instead of placing deterministic constraints on the minimum standoff distance as used in the baseline approach, limits are enforced on the probability of violating those uncertain constraints.

The goal is to jointly constrain the probability of getting too close to the terrain at all points to be less than some threshold, δ. With this, the optimization becomes

$$\begin{aligned} \underset{P}{\text{minimize}} \quad & \|NP - D\| \\ \text{subject to} \quad & \kappa \leq \kappa_{\max} \\ & -\theta_{\max} \leq \theta \leq \theta_{\max} \\ & \mathrm{P}\left(E < 0\right) \leq \delta. \end{aligned} \tag{6}$$

However, this joint multivariate probability distribution is prohibitively computationally complex, so a method to relax the problem is needed to make it computationally feasible for onboard computation. There are a number of common relaxations to separate the joint constraint into a set of individual, independent constraints. The approach selected here is to use Boole's inequality, which states that the sum of the probabilities of the individual events will be greater than or equal to the joint probability of the events. For the problem described above, this becomes

$$\mathrm{P}\left(E < 0\right) = \mathrm{P}\left(\bigcup_k E_k < 0\right) \leq \sum_k \mathrm{P}\left(E_k < 0\right). \tag{7}$$

As a result, this relaxation will overestimate the probability of violating the constraints, giving a trajectory that is conservative on the side of safety.

With the definition of what constitutes unsafe proximity to the terrain given in Equation 5, the probability of violating that minimum can now be constrained as

$$\begin{aligned} \mathrm{P}\left(E_k < 0\right) &\leq \varepsilon_k \\ \sum_k \varepsilon_k &= \delta, \end{aligned} \tag{8}$$

where ε_k is the probability of violating the kth limit, and δ is the total allowable probability of violation. Now the optimization becomes

$$\begin{aligned} \underset{P}{\text{minimize}} \quad & \|NP - D\| \\ \text{subject to} \quad & \kappa \leq \kappa_{\max} \\ & -\theta_{\max} \leq \theta \leq \theta_{\max} \\ & \mathrm{P}\left(E_k < 0\right) \leq \varepsilon_k \\ & \sum_k \varepsilon_k = \delta. \end{aligned} \tag{9}$$

Under the assumption of Gaussian uncertainty in the system, each individual constraint can be written as

$$\mathrm{P}\left(E_k < 0\right) = 1 - \Phi\left(\frac{E_k}{\sigma_k}\right) \leq \varepsilon_k, \tag{10}$$

where $\Phi\left(\cdot\right)$ is the Gaussian CDF and σ_k^2 is the variance of the uncertainty associated with the kth constraint. This function is convex for values of $\varepsilon_k < 0.5$, allowing for rapid solution in the optimization. In order to evaluate this constraint, the uncertainty term, σ_k, must be calculated.

A. Determination of Uncertainty

Capturing the various sources of uncertainty in σ_k is an important part of implementing chance constraints.

By assuming that the spline trajectory and the map are uncorrelated,

$$\sigma_k^2 = \mathrm{var}\left(N_k P - d_{k,\text{min}}\right) \tag{11}$$

can be reduced to

$$\sigma_k^2 = N_k \Sigma_P N_{k_\intercal} + \sigma_{dk}^2. \tag{12}$$

The first component in this equation, Σ_P, is the uncertainty in the location of the spline's control points. Another way to interpret this term is that it represents the amount of uncertainty in the vehicle's ability to follow the trajectory. This captures the stochastic sources of error in the motion of the vehicle, including modeling errors and disturbances such as currents.

The other component of uncertainty, σ_{dk}^2, captures the uncertainty in the knowledge of the terrain. Maps of the terrain are not perfect, with errors arising from averaging as well as small changes to the terrain over time. In addition, the errors that arise from averaging are amplified in exciting terrain. Therefore, the uncertainty from the map is composed of two terms – a baseline noise, σ_{nom}^2, and a term that is calculated based on the variation in the surrounding terrain, σ_{surr}^2.

$$\sigma_{dk}^2 = \sigma_{\text{nom}}^2 + \sigma_{\text{surr}}^2. \tag{13}$$

When planning directly from an *a priori* map, σ_{surr}^2 is computed using map cells in all directions. This takes into

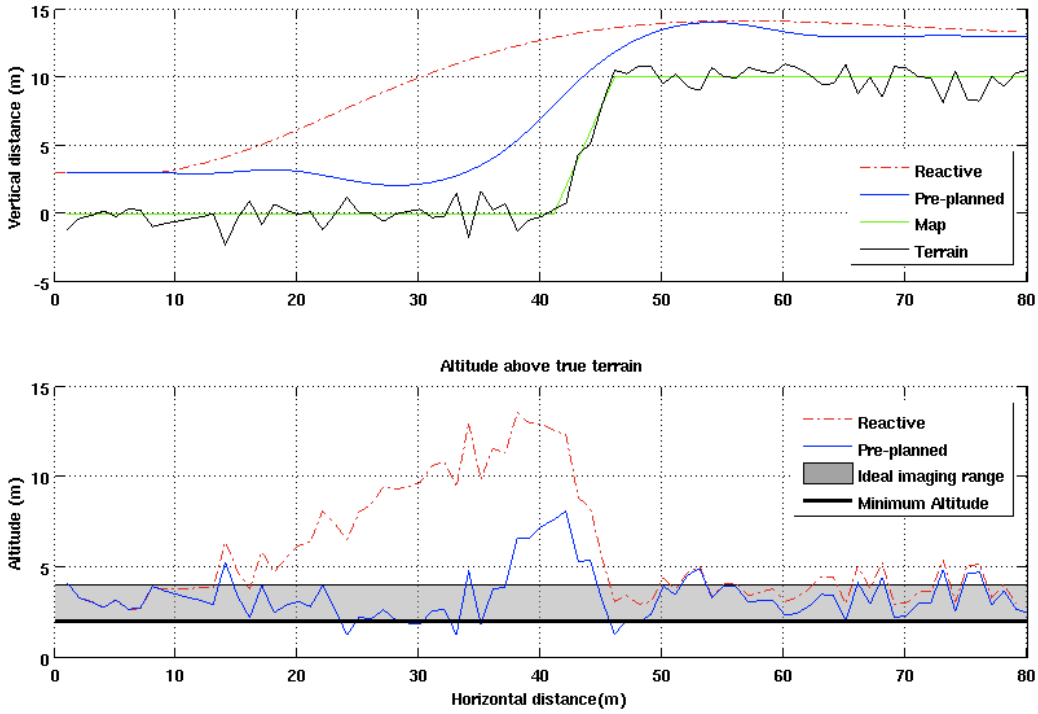

Fig. 4. Reactive trajectory (red dashed line) compared to pre-planned trajectory (solid blue line). The top plot shows the trajectories over the map and the terrain. The lower plot shows the altitude of the trajectories over the true terrain. The pre-planned trajectory has much better performance, staying within the ideal imaging range for significantly more of the trackline.

account errors in the localization of the vehicle with respect to the map. However, when planning a trajectory based on a forward-looking profiling sonar, only along-track data points are available and therefore used to calculate σ^2_{surr}.

The evaluation of uncertainty from Equation 12 can be applied to Equation 10, allowing the constraint of the probability of violating the minimum standoff distance to be implemented.

IV. Results

For the results shown here, trajectories have been planned for an AUV with a 17 meter effective turning radius and a maximum pitch of 45 degrees. The desired standoff distance is 3 meters, and the minimum standoff distance for safety is 2 meters. The ideal imaging range is given as 2-4 meters of altitude.

Similar to work presented previously [6], Figure 4 shows the improvement in performance of a trajectory planned with *a priori* map data over that of the trajectory generated with a reactive approach.

The reactive approach implemented here uses a forward-looking multibeam sonar to sense the terrain ahead of it. The commanded depth is set by the depth of the highest point within a given distance ahead of the vheicle. As a result, as soon as the AUV sees the step in the terrain ahead, it pulls up to ensure safety.

The two trajectories flown by the vehicle traveling from left to right are shown in the top plot of Figure 4 over the map and the terrain, with the reactive trajectory as a red dashed line and the pre-planned trajectory as a blue solid line. The lower plot shows the altitude of the two trajectories over the true terrain. The pre-planned trajectory uses the *a priori* map data and stays closer to the terrain, staying within the ideal imaging range for significantly more of the trajectory, providing much improved performance.

Note that while the pre-planned trajectory in Figure 4 remains above the minimum altitude of 2 meters with respect to the map, it ends up getting closer to the true terrain since the assumption has been made that the map perfectly represents the terrain.

Figure 5 demonstrates the improvement in safety that can be gained by explicitly incorporating knowledge of the uncertainty into the planning of trajectories. For this example, $\delta = 0.15$, $\Sigma_P = 0.2$ meters, $\sigma_{dk} = 0.5$ meters, and the map has Gaussian noise added with a standard deviation of 0.75 meters. Σ_P is left small to highlight the effects of map uncertainty. The top plot of Figure 5 again shows two trajectories over the map and the terrain, with a trajectory planned with no uncertainty shown with a magenta dashed line and a trajectory planned with uncertainty in the terrain shown with a solid blue line.

The lower plot of Figure 5 shows the altitude of the two trajectories over the true terrain. While the trajectory planned without uncertainty violates the minimum altitude of 2 meters, the trajecory planned with knowledge of the terrain uncertainty never comes too close to the terrain.

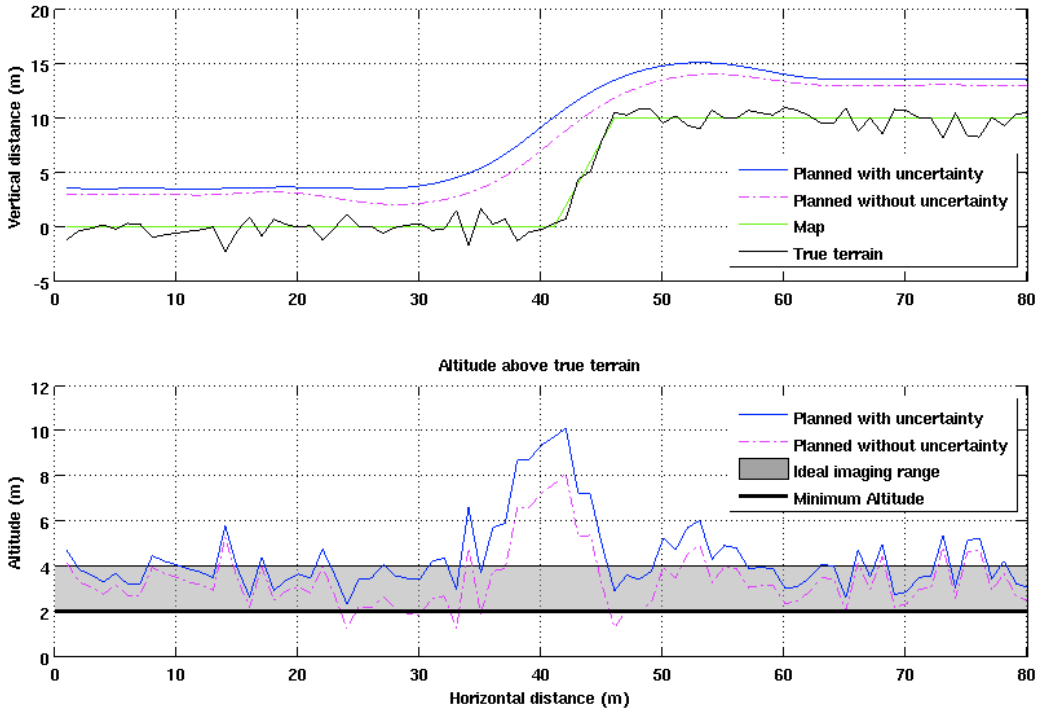

Fig. 5. Trajectories planned with (blue solid line) and without (magenta dashed line) uncertainty. The top plot shows the two trajectories plotted over the map and the true terrain. The lower plot shows the altitude of the two trajectories over the true terrain. The trajectory planned with no uncertainty spends more time in the ideal imaging range, but violates the minimum altitude.

Including uncertainty in the trajectory optimization results in improved safety for the vehicle, there is a tradeoff with the potential loss of performance, with the AUV spending more time outside of the ideal imaging range. This is the fundamental trade in planning trajectories using uncertainty – giving up some performance in order to have increased safety by being more robust to uncertainties in the environment. The approach presented here explicitly minimizes the potential loss of performance while achieving the desired degree of safety.

V. Conclusions

This work demonstrates an effective way of incorporating known sources of uncertainty into the process of planning aggressive, terrain-following trajectories. The constrained optimization provides a trade off between safety and performance by explicitly incorporating uncertainty into the safety constraints. Trajectories that are planned without incorporating uncertainty can end up too close to the terrain, while those that take the sources of uncerainty into account are more robust, but have a corresponding reduction in performance as they spend more time outside the ideal imaging range.

Acknowledgements

The authors would like to thank MBARI for support. This work was supported in part under NASA ASTEP Grant NNX11AR62G.

References

[1] O. Hagen, K. Anonsen, and T. Saebo, "Low altitude AUV terrain navigation using an interferometric sidescan sonar," in *OCEANS 2011*, sept. 2011, pp. 1 –8. [Online]. Available: http://ieeexplore.ieee.org/xpls/abs_all.jsp?arnumber=6107003

[2] D. Meduna, "Terrain relative navigation for sensor-limited systems with application to underwater vehicles," PhD, Stanford University, August 2011. [Online]. Available: http://purl.stanford.edu/mq108ss0503

[3] I. Nygren, "Robust and efficient terrain navigation of underwater vehicles," in *Position, Location and Navigation Symposium, 2008 IEEE/ION*, may 2008, pp. 923 –932.

[4] V. Creuze and B. Jouvencel, "Avoidance of underwater cliffs for autonomous underwater vehicles," in *Intelligent Robots and Systems, 2002. IEEE/RSJ International Conference on*, vol. 1. IEEE, 2002, pp. 793–798.

[5] A. Bennett, J. Leonard, and J. Bellingham, "Bottom following for survey-class autonomous underwater vehicles," in *International Symposium on Unmanned Untethered Submersible Technology*. UNIVERSITY OF NEW HAMPSHIRE-MARINE SYSTEMS, 1995, pp. 327–336.

[6] S. E. Houts, S. M. Rock, and R. McEwen, "Aggressive terrain following for motion-constrained AUVs," in *IEEE AUV 2012*, Southampton, England, 09/2012 2012. [Online]. Available: https://www.stanford.edu/group/arl/sites/default/files/public/publications/HoutsRM2012.pdf

[7] M. P. Vitus, "Stochastic control via chance constrained optimization and its application to unmanned aerial vehicles," Ph.D. dissertation, Stanford University, March 2012.

[8] L. Piegl and W. Tiller, *The NURBS Book*. Springer Berlin, 1997.